Gates for one-way quantum computation based on Einstein-Podolsky-Rosen entanglement

Shuhong Hao, Xiaowei Deng, Xiaolong Su* and Xiaojun Jia, Changde Xie, and Kunchi Peng
State Key Laboratory of Quantum Optics and Quantum Optics Devices,
Institute of Opto-Electronics, Shanxi University, Taiyuan, 030006, People's Republic of China

Single-mode squeezing and Fourier transformation operations are two essential logical gates in continuous-variable quantum computation, which have been experimentally implemented by means of an optical four-mode cluster state. In this paper, we present a simpler and more efficient protocol based on the use of Einstein-Podolsky-Rosen two-mode entangled states to realize the same operations. The theoretical calculations and the experimental results demonstrate that the presented scheme not only decreases the requirement to the resource quantum states at the largest extent but also enhances significantly the squeezing degree and the fidelity of the resultant modes under an identical resource condition. That is because in our system the influence of the excess noises deriving from the imperfect squeezing of the resource states is degraded. The gate operations applying two-mode entanglement can be utilized as a basic element in a future quantum computer involving a large-scale cluster state.

PACS numbers: 03.67.Lx, 42.50.Dv

arXiv:1403.2490v1 [quant-ph] 11 Mar 2014

I. INTRODUCTION

Over the past few decades a variety of fundamental protocols for implementing quantum computation (QC) have been explored [1, 2]. There are two different models in the QC regime, which are the traditional circuit model, in which unitary evolution and coherent control of individual qubits are required [1], and the cluster model, in which the logical operations are achieved through measurements and classical feedforward of measured results on a cluster entangled state [3]. Due to the role of measurements the QC based on cluster entanglement is essentially irreversible, and thus it is named the one-way QC [3]. The one-way QC was first experimentally demonstrated with a four-qubit cluster state of single photons [4–6]. In the meanwhile, an universal QC model using continuous-variable (CV) cluster states was proposed [7]. Applying the approach of quantum optics, CV cluster states of optical field can be unconditionally prepared [8–11], and the one-way CVQC can be deterministically performed [7, 12]. Therefore, the probabilistic problems existing in most qubit information systems of single photons [4–6] can be overcome. It has been theoretically and experimentally demonstrated that one-mode linear unitary Bogoliubov (LUBO) transformations corresponding to Hamiltonians that are quadratic in quadrature amplitude and phase operators of quantized optical modes (qumodes) can be implemented using a four-mode linear cluster state [13, 14]. At the same time, the Deutsch-Jozsa algorithm for CVQC has been proposed [15]. Following the theoretical proposals, the different logical gates used for CVQC were experimentally realized. First, a quantum nondemolition sum gate and a quadratic phase gate for one-way CVQC were demonstrated based on utilizing squeezed states of light by Furusawa's group in 2008 and 2009, respectively [16, 17]. Successively, a controlled-X gate based on a four-mode optical CV cluster state was presented by Peng's group, in which a pair of quantum teleportation elements were used for the transformation of quantum states from input target and control states to output states [18]. Later, the squeezing operation, Fourier transformation and controlled-phase gate were also achieved by Ukai et al., in which four-mode optical cluster states served as resource quantum states [14, 19].

Here, we present a measurement-based logical operation scheme with which the squeezing and Fourier transformations for a single qumode can be implemented using an Einstein-Podolsky-Rosen (EPR) entangled state as the resource. These operations can be achieved on a fixed experimental system only by choosing appropriate measurement angles in homodyne detections. Since EPR entanglement of optical modes is deterministic and homodyne detections can be well controlled, the presented CVQC gates are operated in a completely unconditional and controllable version. By changing the quadrature measurement angles of homodyne detections the squeezing operations at three different squeezing levels (-4, -8, -12 dB) and Fourier transformation are experimentally performed. The experimental results and the corresponding theoretical expectations are in good agreement. As is well known, the EPR entanglement is equivalent to a two-mode cluster state [8], and thus, QC using an EPR state can be implemented on two submodes of a large cluster state as a step of a full one-way CVQC. We also prove that the squeezing degree and the fidelity of the output mode obtained by using an EPR state are better than that obtained using a four-mode cluster state if the squeezing of the initial resource state is identical. That is because the excess noises deriving from imperfect squeezing of the resource state in the EPR system are less than that in the four-mode cluster state system. Theore-

*Electronic address: suxl@sxu.edu.cn

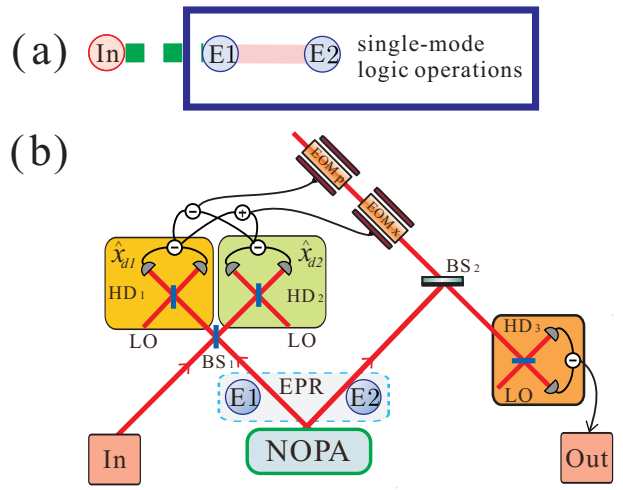

FIG. 1: (Color online) The schematic of a single-mode quantum logic operation with an EPR entangled state. (a): the graph representation, (b): experimental set-up. The input state α is coupled to an EPR entangled state E1-E2 via a 50% beam-splitter BS_1. Measurement results from two homodyne detection systems (HD_1 and HD_2) are fedforward to modes E2. The output mode is measured by HD_3. LO: local ossilator for the homodyne detection. EOMx and EOMp: amplitude and phase electro-optical modulators. BS_2: a mirror with 99% reflection coefficient.

fore, the presented CVQC schemes not only decrease the requirement to quantum resource and simplify the experimental system significantly but also enhance the quality of the output states. Finally, we point out that the set-up can be applied to perform a cascaded operation of a squeezing gate and a Fourier gate by changing the relative phase between the input mode and a submode of the EPR state, which shows further the diversity of the protocol.

II. PROTOCOL AND PRINCIPLE OF QUANTUM LOGICAL OPERATIONS

The single-mode squeezing gate in CVQC depending on quantized optical modes is expressed by $\hat{S}(r) = e^{ir(\hat{x}\hat{p}+\hat{p}\hat{x})}$, where r is the squeezing parameter, $\hat{x} = (\hat{a}+\hat{a}^\dagger)/2$ and $\hat{p} = (\hat{a}-\hat{a}^\dagger)/2i$ are the amplitude and phase quadratures of an optical mode $\hat{a}$, respectively. The input-output relation of the squeezing gate is written as $\hat{\xi}_j = \mathbf{S}\hat{\xi}_j$, where $\hat{\xi}_j = (\hat{x}_j, \hat{p}_j)^T$ and

$$\mathbf{S} = \begin{pmatrix} e^r & 0 \\ 0 & e^{-r} \end{pmatrix} \tag{1}$$

represents the squeezing operation of the phase quadrature.

Fig. 1 shows a schematic of the single-mode squeezing and Fourier transformation gate based on applying an EPR entangled state, (a) is the graph representation, (b) is the experimental set-up. An input mode is coupled to a submode of the EPR entangled state (E1) via a 50% beam-splitter BS_1. The two output modes of BS_1 are measured by homodyne detection systems HD_1 and HD_2, respectively. The measured results are fedforward to the other submode of the EPR entangled state (E2) by classical feedforward circuits and electro-optical modulators (EOM). The sum (+) and difference (−) of the photocurrents measured by HD_1 and HD_2 are only used for the single-mode squeezing gate. When Fourier transformation is implemented, they are not utilized. The resultant optical mode is measured by the third homodyne detection system HD_3.

In the standard CV quantum teleportation process [20], the amplitude and phase quadratures of output modes from BS_1 are measured by two homodyne detection systems, the measurement angles of which are chosen as 0 and $\pi/2$, respectively. However, in the presented quantum logic operation the measurement angle will be chosen arbitrarily, and the squeezing degree of the squeezing gate will be determined by the measurement angle. Thus, we can say that the CVQC logic operation is implemented by means of a CV quantum teleportation process with an arbitrarily chosen measurement angle.

If the input mode is coupled to mode E_1 with a $\pi/2$ phase difference on BS_1, the measurement results of HD_1 and HD_2, $\hat{x}_{d1}$ and $\hat{x}_{d2}$, are expressed by

$$\begin{aligned} \hat{x}_{d1} &= \frac{\cos\theta_1(\hat{x}_{in}-\hat{p}_1)+\sin\theta_1(\hat{p}_{in}+\hat{x}_1)}{\sqrt{2}}, \\ \hat{x}_{d2} &= \frac{\cos\theta_2(\hat{x}_{in}+\hat{p}_1)+\sin\theta_2(\hat{p}_{in}-\hat{x}_1)}{\sqrt{2}}, \end{aligned} \tag{2}$$

where θ_1 and θ_2 are the measurement angles of HD_1 and HD_2, respectively. Choosing $\theta_2 = -\theta_1$, the amplitude and phase quadratures of the resultant mode equal to:

$$\begin{aligned} \begin{pmatrix} \hat{x}_{out} \\ \hat{p}_{out} \end{pmatrix} &= \begin{pmatrix} \hat{x}_2 \\ \hat{p}_2 \end{pmatrix} + G_S \begin{pmatrix} \hat{x}_{d1} \\ \hat{x}_{d2} \end{pmatrix} \\ &= \begin{pmatrix} \cot\theta_1 & 0 \\ 0 & \tan\theta_1 \end{pmatrix} \begin{pmatrix} \hat{x}_{in} \\ \hat{p}_{in} \end{pmatrix} + \begin{pmatrix} \hat{\delta}_1 \\ -\hat{\delta}_2 \end{pmatrix}, \end{aligned} \tag{3}$$

where

$$G_S = \begin{pmatrix} \frac{1}{\sqrt{2}\sin\theta_1} & \frac{1}{\sqrt{2}\sin\theta_1} \\ \frac{1}{\sqrt{2}\cos\theta_1} & \frac{-1}{\sqrt{2}\cos\theta_1} \end{pmatrix} \tag{4}$$

is the corresponding gain factor and $\hat{\delta}_1 = \hat{x}_1 + \hat{x}_2$ and $\hat{\delta}_2 = \hat{p}_1 - \hat{p}_2$ are the excess noises of the amplitude and phase quadratures of the EPR entangled state respectively, which result from the imperfect entanglement of the resource state and whose variances depend on the squeezing parameter r_E of the EPR state by $\langle\Delta^2(\hat{x}_1+\hat{x}_2)\rangle = \langle\Delta^2(\hat{p}_1-\hat{p}_2)\rangle = e^{-2r_E}/2$. For an ideal EPR state $r_E \to \infty$ and thus $\hat{\delta}_1 = \hat{\delta}_2 = 0$. The ideal EPR state does not exist really since it requires infinite energy [7].

Comparing Eq. (3) in the case of ideal EPR state with Eq. (1), we can see that the transformation corresponds to a single-mode amplitude and phase squeezing

gate with $\cot\theta_1 = e^{-r}$ and e^r, respectively. In this case, the transformation matrix is given by

$$\mathbf{S} = \begin{pmatrix} \cot\theta_1 & 0 \\ 0 & \tan\theta_1 \end{pmatrix}. \tag{5}$$

Equation (5) shows that the squeezing parameter r depends on the measurement angles. When the measurement angle is varied from 45° to 0° the squeezing degree of the squeezing gate increases from 0 to $-\infty$. The squeezing level can be controlled by choosing different measurement angles. The measurement angles (θ_1, θ_2) for the squeezing levels of -4, -8, and -12 dB are $(32.25°, -32.25°)$, $(21.70°, -21.70°)$, and $(14.10°, -14.10°)$, respectively.

When we take $\theta_1 = 0$ and $\theta_2 = -\pi/2$, the amplitude and phase quadratures of the resultant mode are

$$\begin{aligned} \begin{pmatrix} \hat{x}_{out} \\ \hat{p}_{out} \end{pmatrix} &= \begin{pmatrix} \hat{x}_2 \\ \hat{p}_2 \end{pmatrix} + G_F \begin{pmatrix} \hat{x}_{d1} \\ \hat{x}_{d2} \end{pmatrix} \\ &= \mathbf{F} \begin{pmatrix} \hat{x}_{in} \\ \hat{p}_{in} \end{pmatrix} + \begin{pmatrix} \hat{\delta}_1 \\ -\hat{\delta}_2 \end{pmatrix}, \end{aligned} \tag{6}$$

where

$$G_F = \begin{pmatrix} 0 & \sqrt{2} \\ \sqrt{2} & 0 \end{pmatrix} \tag{7}$$

is the corresponding gain factor of the feedforward circuit. The transformation matrix $\mathbf{F} = \begin{pmatrix} 0 & -1 \\ 1 & 0 \end{pmatrix}$ just corresponds to a Fourier transformation. Thus, a Fourier transformation operation can also be implemented with the experimental system of Fig. 1 (b) only by choosing appropriate measurement angles and feedforward circuit.

In the one-way quantum computation scheme with the four-mode cluster state as the resource , the excess noises of the amplitude ($\hat{\delta}_{xc}$) and phase ($\hat{\delta}_{pc}$) quadratures of the output mode for the squeezing of a dB ($a < 0$ and $a > 0$ correspond to phase squeezing and amplitude squeezing, respectively) are given by [14]

$$\begin{pmatrix} \hat{\delta}_{xc} \\ \hat{\delta}_{pc} \end{pmatrix} = \begin{pmatrix} \frac{1}{\sqrt{2}} e^{-r_c} \hat{p}_1^0 - \sqrt{\frac{5}{2}} e^{-r_c} \hat{p}_2^0 \\ -\sqrt{\frac{5}{2}} e^{-r_c} \hat{p}_3^0 + \frac{1}{\sqrt{2}} e^{-r_c} \hat{p}_4^0 \end{pmatrix} \tag{8}$$

when $V = 10^{a/10} \leq \frac{3}{2}$, and

$$\begin{pmatrix} \hat{\delta}_{xc} \\ \hat{\delta}_{pc} \end{pmatrix} = \begin{pmatrix} \frac{e^{-r_c}\left[3\hat{p}_1^0/V - 2\sqrt{5}\hat{p}_2^0 + \sqrt{2V-3}\left(\sqrt{5}\hat{p}_3^0 + \hat{p}_4^0\right)/V\right]}{2\sqrt{2}} \\ \frac{e^{-r_c}\left[\sqrt{2V-3}\hat{p}_1^0 - \sqrt{5}\hat{p}_3^0 + \hat{p}_4^0\right]}{\sqrt{2}} \end{pmatrix} \tag{9}$$

when $V > \frac{3}{2}$, where r_c is the squeezing parameter of four phase squeezed state $\hat{p}_{1-4}$, and the superscript 0 represents the vacuum mode. From Eq. (8) we can calculate the variance of the excess noise for phase squeezing: $\left\langle \Delta^2 \hat{\delta}_{xc} \right\rangle = \left\langle \Delta^2 \hat{\delta}_{pc} \right\rangle = 3e^{-2r_c}/4$, where the noise variance of the vacuum mode is normalized to $\left\langle \Delta^2 \hat{x}^0 \right\rangle = \left\langle \Delta^2 \hat{p}^0 \right\rangle = 1/4$. In our scheme the variance of the excess noise is the quantum correlation variances of the EPR entangled state [21], i.e. $\left\langle \Delta^2(\hat{x}_1 + \hat{x}_2) \right\rangle = \left\langle \Delta^2(\hat{p}_1 - \hat{p}_2) \right\rangle = e^{-2r_E}/2$. Comparing the two cases, we find that the variances of the excess noises in the scheme using the EPR resource state is 2/3 of that using a four-mode cluster state if the squeezing degree of the initial resource squeezed state is the same.

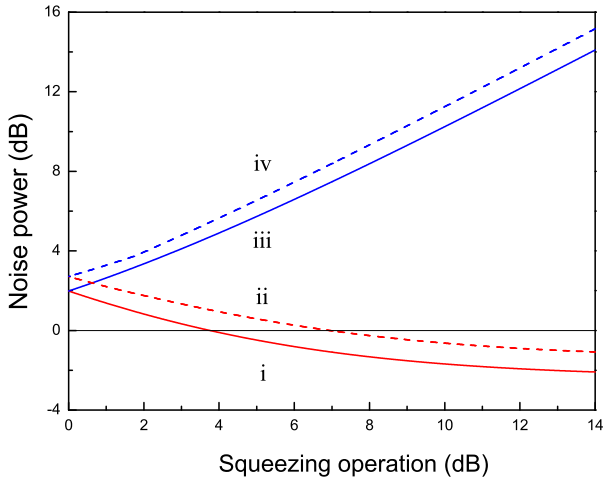

FIG. 2: (Color online) The dependence of the noise power of the output mode on the amplitude squeezing level of the squeezing operation for different resource states. Input state: a vacuum state. Traces i and iii (solid lines) correspond to squeezed and antisqueezed noises using an EPR entangled state as a resource state, respectively. Traces ii and iv (dashed lines) correspond to squeezed and antisqueezed noises with a four-mode cluster state as resource state, respectively. The initial resource squeezing is -5.3 dB for the two cases.

Fig. 2 compares the noise powers of the output modes of the amplitude squeezing operation implemented in the two systems using the EPR entangled state (solid lines) and the four-mode cluster state (dashed lines) as resource states, in which the initial squeezing of the resource states is taken to be the same (-5.3 dB). The noise power is calculated by $10\log_{10}[B/B_0]$ dB, where B represents the noise variance of the quadrature component and $B_0 = 1/4$ is the normalized vacuum noise. In this case, 0 dB in Fig. 2 corresponds to the vacuum noise level. It is obvious that both squeezed (traces i and ii) and antisqueezed (traces iii and iv) noise powers of the output modes obtained by the system using the EPR entangled state are lower than those obtained by the system using the four-mode cluster state in Ref. [14]. Therefore, for a given initial squeezing resource, the squeezing gate based on EPR entanglement can generate the squeezed states with a higher squeezing degree and lower antisqueezing noises than that obtained using the four-mode cluster state.

III. EXPERIMENTAL SET-UP AND RESULTS

A. Experimental set-up

The experimental set-up is shown in Fig. 1 (b). The non-degenerate optical parametric amplifier (NOPA) is pumped by a continuous wave intra-cavity frequency-doubled and frequency-stabilized Nd:YAP-LBO (Nd-doped $YAlO_3$ perovskite-lithium triborate) laser with two output wavelengths at 540 nm and 1080 nm [22]. The NOPA consists of an α-cut type-II potassium titanyl phosphate (KTP) crystal and a concave mirror [21]. The front face of the KTP crystal is coated to be used for the input coupler and the concave mirror serves as the output coupler of the squeezed states. The transmissions of the input (output) coupler at 540 and 1080 nm are 99.8% (0.5%) and 0.04% (5.2%), respectively. The EPR entangled states at 1080 nm are generated via the frequency-down-conversion process of the pump field at 540 nm inside the NOPA. The amplitude anti-correlated ($\hat{x}_1 + \hat{x}_2 \to 0$) and phase correlated ($\hat{p}_1 - \hat{p}_2 \to 0$) EPR entangled optical beams are obtained when the NOPA is operated at the deamplification condition, which corresponds to locking the relative phase between the pump laser and the injected signal to $(2n+1)\pi$ (n is the integer) [21]. The experimentally measured squeezing of the EPR entangled state is about -4.0 dB.

B. Squeezing operation

Fig. 3 (a) and (b) show the output noise power of the -12 dB phase squeezing operation with a vacuum input and a $\hat{p}$-coherent input, respectively. Trace i (black line) is the shot-noise-level (SNL); traces ii and iii (red and blue lines) are the squeezed and anti-squeezed noises, respectively. Although in the ideal case with $\hat{\delta}_1 = \hat{\delta}_2 = 0$, the input vacuum state should be squeezed -12 dB, in the practical experiment the input vacuum mode is squeezed 0.6 dB below the corresponding SNL due to the influence of the excess noises introduced by the imperfect EPR entanglement.

In order to test the generality of the squeezing operation, we implement a squeezing operation on a $\hat{p}$-coherent input state with a modulation signal of 20 dB on its phase quadratures. In Fig. 3 (b), trace ii (green line) stands for the input coherent state. The squeezing (trace iv) and anti-squeezing (trace iii) noise levels of the output mode are 8.2 dB and 12.2 dB above the SNL, respectively. Fig. 3 (c) shows the three different squeezing levels (-4, -8, and -12 dB) with a vacuum state (trace ii and iii) and a $\hat{p}$-coherent state (trace iv) as input states, respectively. The measurement results agree well with the theoretical curves (solid lines).

Besides the squeezed noise level of the output mode, we also use the fidelity $F = \left\{\mathrm{Tr}[(\sqrt{\hat{\rho}_1}\hat{\rho}_2\sqrt{\hat{\rho}_1})^{1/2}]\right\}^2$, which denotes the overlap between the experimentally obtained output state $\hat{\rho}_2$ and the ideal output sate $\hat{\rho}_1$, to quantify the performance of the squeezing operation. The fidelity for two Gaussian states $\hat{\rho}_1$ and $\hat{\rho}_2$ with covariance matrices $\mathbf{A}_j$ and mean amplitudes $\alpha_j \equiv (\alpha_{jx}, \alpha_{jp})$ $(j = 1, 2)$ is expressed as [23, 24]

$$F = \frac{2}{\sqrt{\Delta + \sigma} - \sqrt{\sigma}} \exp[-\beta^T (\mathbf{A}_1 + \mathbf{A}_2)^{-1} \beta], \qquad (10)$$

where $\Delta = \det(\mathbf{A}_1 + \mathbf{A}_2)$, $\sigma = (\det \mathbf{A}_1 - 1)(\det \mathbf{A}_2 - 1)$, $\beta = \alpha_2 - \alpha_1$, and $\mathbf{A}_1$ and $\mathbf{A}_2$ are for the ideal ($\hat{\rho}_1$) and experimental ($\hat{\rho}_2$) output states, respectively. The covariance matrices $\mathbf{A}_j$ $(j = 1, 2)$ for the target mode are given by

$$\mathbf{A}_{out1} = 4 \begin{bmatrix} \left\langle \Delta^2 \hat{x}_{out} \right\rangle_1 & 0 \\ 0 & \left\langle \Delta^2 \hat{p}_{out} \right\rangle_1 \end{bmatrix}, \qquad (11)$$

$$\mathbf{A}_{out2} = 4 \begin{bmatrix} \left\langle \Delta^2 \hat{x}_{out} \right\rangle_2 & 0 \\ 0 & \left\langle \Delta^2 \hat{p}_{out} \right\rangle_2 \end{bmatrix}. \qquad (12)$$

The coefficient 4 comes from the normalization of the SNL. Since the noise of a vacuum state is defined as 1/4 above, while in the fidelity formula the vacuum noise is normalized to 1, a coefficient 4 appears in the expressions of covariance matrices. In the case of infinite squeezing, the fidelity for the output state equals 1, which can be calculated from Eq. (3) with $\hat{\delta}_1 = \hat{\delta}_2 = 0$ $(r \to \infty)$.

Fig. 4 shows the fidelity as a function of the phase squeezing. We can see that the fidelity with the -4.0 dB EPR state as a resource state (trace i, blue solid line) is higher than the classical limit which is obtained by using the coherent state to substitute for the EPR state (trace iii, blue dashed line). For the comparison, we calculate the fidelity based on the four-mode cluster state with the same initial squeezing resource of -4.0 dB. Traces ii (red line) and iv (red dash) are the fidelities with and without four-mode cluster state (-4.0 dB initial squeezing) as a resource state. The fidelity of squeezing operation using the EPR state as a resource state is higher than that using the four-mode cluster state. This is because the excess noise deriving from the squeezing operation in the scheme using the EPR state is only 2/3 of that based on the four-mode cluster state [14]. Experimentally measured data are marked on the graph with black dots, which are in good agreement with the theoretical expectation.

C. Fourier operation

It has been theoretically proved in section II that when the measurement angles of HD_1 and HD_2 are taken as 0 and $\pi/2$, respectively, the input mode will complete the Fourier transformation via a teleportation process in the experimental system of Fig. 1(b). Fig. 5 shows the experimental results of Fourier transformation with a coherent input. Figures 5(a) and 5(b) correspond to noise powers of the input and output states, respectively. Trace

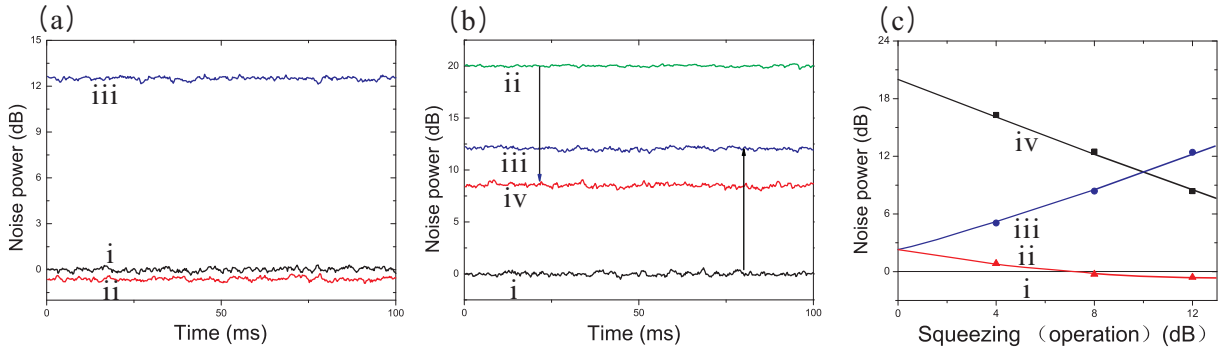

FIG. 3: (Color online) The experimental results of the single-mode squeezing operation. (a): the −12 dB squeezing operation with a vacuum input state, (b): −12 dB squeezing operation with a $\hat{p}$-coherent state. Trace i: SNL, traces ii: input variances of the $\hat{p}$-coherent state, traces iii and iv: anti-squeezing and squeezing noise. (c): experimental results (dots) and theoretical curves (lines) for −4, −8 and −12 dB squeezing operation. Traces ii and iii: squeezing and anti-squeezing with a vacuum state, trace iv: squeezing for a $\hat{p}$-coherent state. Measurement frequency: 2 MHz, parameters of the spectrum analyzer: resolution bandwidth: 30kHz, video bandwidth: 100Hz.

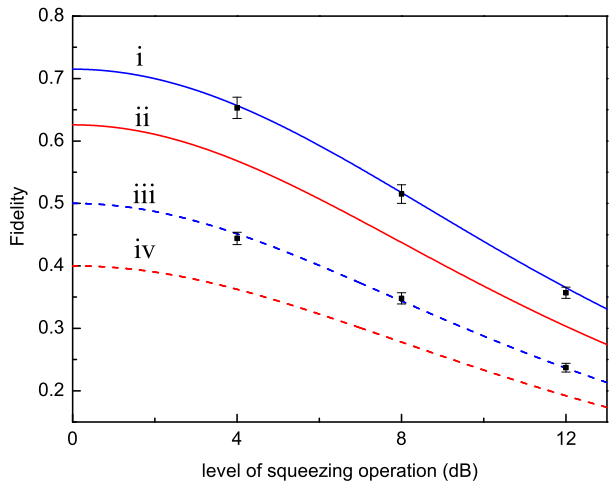

FIG. 4: (Color online) The fidelity as a function of phase-squeezing. Traces i and iii are fidelities with and without EPR entanglement as a resource, respectively. Traces ii and iv are fidelities with and without a four-mode cluster state as a resource, respectively. The initial resource squeezing is −4.0 dB for traces i and ii.

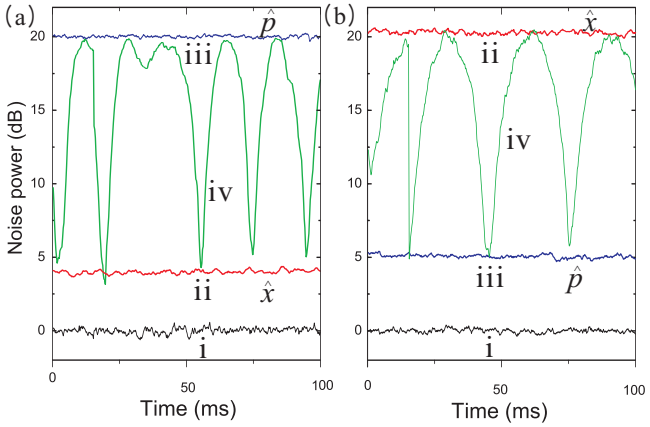

FIG. 5: (Color online) The experimental results of Fourier transformation. (a): input state, (b): output state. Trace i: SNL, traces ii and iii: amplitude and phase quadratures, respectively. Trace iv: noise power when the phase of the homodyne detection system is scanned. Measurement frequency: 2 MHz, parameters of the spectrum analyzer: resolution bandwidth: 30kHz, video bandwidth: 100Hz.

i (black line) is the SNL, and traces ii and iii (red and blue lines) stand for the average noise levels of the amplitude and phase quadratures of the input [Fig.5(a)] and output [Fig. 5(b)] modes, respectively. Trace iv (green line) is the noise power spectrum of the input [Fig. 5(a)] and output [Fig. 5(b)] states measured by scanning the phase of the homodyne detection system. A coherent state with a 4 dB amplitude modulation signal on the amplitude quadrature and a 20 dB amplitude modulation signal on the phase quadrature is used for the input state [Fig.5 (a)]. Fig. 5 (b) shows the amplitude and phase quadratures of the output state after the Fourier transformation. Comparing Figures 5(a) and 5(b), we can see that the input mode has been rotated 90° in the phase space, and thus, the Fourier transformation from the phase (amplitude) quadrature to the amplitude (phase) quadrature has been achieved.

IV. CONCLUSION

In conclusion, we have designed and experimentally demonstrated two essential one-mode LUBO transformations based on the use of an EPR entangled state. Squeezing and Fourier transformation operations are implemented on an experimental set-up. These operations are easily controlled by adjusting the phase of the local

oscillator in the homodyne detectors. The calculation accuracy of one-way CVQC depends on the initial resource squeezing since an imperfect resource state will introduce excess noises into the calculated resultant states via the gate operations. The excess noises deriving from the EPR system are less than those from the four-mode cluster system, so better accuracy can be obtained by the gates using EPR entanglement under the condition of applying the same initial squeezing resource.

Finally, we demonstrate theoretically that the presented experimental set-up can also complete a cascaded single-mode logic operation consisting of a squeezing operation and a Fourier transformation, which shows further the versatility of the system. If the phase difference between the input mode and a submode of the EPR entangled state on BS_1 is taken as zero, the measurement results from the two homodyne detection systems will be

$$\begin{aligned} \hat{x}_{d1} &= \frac{\cos\theta_1(\hat{x}_{in}-\hat{x}_1)+\sin\theta_1(\hat{p}_{in}-\hat{p}_1)}{\sqrt{2}}, \\ \hat{x}_{d2} &= \frac{\cos\theta_2(\hat{x}_{in}+\hat{x}_1)+\sin\theta_2(\hat{p}_{in}+\hat{p}_1)}{\sqrt{2}}. \end{aligned} \quad (13)$$

Choosing $\theta_2 = -\theta_1$, the quadrature components of the output mode equal to

$$\begin{aligned} \begin{pmatrix}\hat{x}_{out}\\ \hat{p}_{out}\end{pmatrix} &= \begin{pmatrix}\hat{x}_2\\ \hat{p}_2\end{pmatrix} + G_{FS}\begin{pmatrix}\hat{x}_{d1}\\ \hat{x}_{d2}\end{pmatrix} \\ &= \begin{pmatrix}0 & -1\\ 1 & 0\end{pmatrix}\begin{pmatrix}\cot\theta_1 & 0\\ 0 & \tan\theta_1\end{pmatrix}\begin{pmatrix}\hat{x}_{in}\\ \hat{p}_{in}\end{pmatrix} + \begin{pmatrix}\hat{\delta}_1\\ -\hat{\delta}_2\end{pmatrix}, \end{aligned} \quad (14)$$

which stands for a cascaded squeezing operation followed by a Fourier transformation, where

$$G_{FS} = \begin{pmatrix}\frac{-1}{\sqrt{2}\cos\theta_1} & \frac{1}{\sqrt{2}\cos\theta_1}\\ \frac{1}{\sqrt{2}\sin\theta_1} & \frac{1}{\sqrt{2}\sin\theta_1}\end{pmatrix} \quad (15)$$

is the corresponding gain factor. Eq. (14) can also be written as

$$\begin{pmatrix}\hat{x}_{out}\\ \hat{p}_{out}\end{pmatrix} = \begin{pmatrix}-\tan\theta_1 & 0\\ 0 & \cot\theta_1\end{pmatrix}\begin{pmatrix}\hat{x}_{in}\\ \hat{p}_{in}\end{pmatrix} + \begin{pmatrix}\hat{\delta}_1\\ -\hat{\delta}_2\end{pmatrix}. \quad (16)$$

Equation (16) means that the squeezing operation followed by a Fourier transformation is equivalent to rotating the measurement angle of the homodyne detection in the squeezing gate by 90°, and thus, the two operations can be achieved in one step. The excess noise induced by imperfect resource squeezing only equals to that of a squeezing gate.

Although two essential single-mode LUBO transformations have been realized by the EPR system, to implement high-order and universal one-way QC, large-scale cluster states and additional non-Gaussian operations are required [7]. However, the presented schemes can be utilized as the basic modules in a full quantum computer using CV cluster entanglement. Saving quantum resources and decreasing excess noise are two favorite features of the EPR system for building a practicable one-way quantum computer with continuous quantum variables of optical modes.

Acknowledgments

This research was supported by the National Basic Research Program of China (Grant No. 2010CB923103), NSFC (Grant Nos. 11174188, 61121064), OIT and Shanxi Scholarship Council of China (Grant No. 2012-010).

[1] M. A. Nielsen and I. L. Chuang, *Quantum computation and Quantum information* (Cambridge University Press, Cambridge, 2000).
[2] A. Furusawa and P. van Loock, *Quantum Teleportation and Entanglement* (Wiley-VCH, Berlin, 2011).
[3] R. Raussendorf, and H. J. A. Briegel, Phys. Rev. Lett. **86**, 5188-5191 (2001).
[4] P. Walther, K. J. Resch, T. Rudolph, E. Schenck, H. Weinfurter, V. Vedral, M. Aspelmeyer, and A. Zeilinger, Nature, **434**, 169 (2005).
[5] R. Prevedel, P. Walther, F. Tiefenbacher, P. Böhi, R. Kaltenbaek, T. Jennewein and A. Zeilinger, Nature, **445**, 65 (2007).
[6] K. Chen, C. M. Li, Q. Zhang, Y. A. Chen, A. Goebel, S. Chen, A. Mair, and J. W. Pan, Phys. Rev. Lett. **99**, 120503 (2007).
[7] N. C. Menicucci, P. van Loock, M. Gu, C. Weedbrook, T. C. Ralph, and M. A. Nielsen, Phys. Rev. Lett. **97**, 110501 (2006).
[8] J. Zhang, and S. L. Braunstein, Phys. Rev. A **73**, 032318 (2006).
[9] P. van Loock, C. Weedbrook and M. Gu, Phys. Rev. A **76**, 032321 (2007).
[10] X. Su, A. Tan, X. Jia, J. Zhang, C. Xie, and K. Peng, Phys. Rev. Lett. **98**, 070502 (2007).
[11] M. Yukawa, R. Ukai, P. van Loock, and A. Furusawa, Phys. Rev. A **78**, 012301 (2008).
[12] C. Weedbrook, S. Pirandola, R. García-Patrón, N. J. Cerf, T. C. Ralph, J. H. Shapiro, and S. Lloyd, Rev. Mod. Phys. **84**, 621 (2012).
[13] R. Ukai, J. I. Yoshikawa, N. Iwata, P. van Loock, and A. Furusawa, Phys. Rev. A **81**, 032315 (2010).
[14] R. Ukai, N. Iwata, Y. Shimokawa, S. C. Armstrong, A. Politi, J. I. Yoshikawa, P. van Loock, and A. Furusawa, Phys. Rev. Lett. **106**, 240504 (2011).
[15] M. Zwierz, C. A. Pérez-Delgado, and P. Kok, Phys. Rev. A **82**, 042320 (2010).
[16] J. I. Yoshikawa, Y. Miwa, A. Huck, U. L. Andersen, P. van Loock, and A. Furusawa, Phys. Rev. Lett. **101**, 250501 (2008).

[17] Y. Miwa, J. I. Yoshikawa, P. van Loock, and A. Furusawa, Phys. Rev. A **80**, 050303(R) (2009).
[18] Y. Wang, X. Su, H. Shen, A. Tan, C. Xie, and K. Peng, Phys. Rev. A **81**, 022311 (2010).
[19] R. Ukai, S. Yokoyama, J. I. Yoshikawa, P. van Loock, and A. Furusawa, Phys. Rev. Lett. **107**, 250501 (2011).
[20] A. Furusawa, J. L. Sorenson, S. L. Braunstein, C. A. Fuchs, H. J. Kimble, and E. S. Polzik, Science **282**, 706 (1998).
[21] Y. Wang, H. Shen, X. Jin, X. Su, C. Xie, and K. Peng, Opt. Express **18**, 6149-6155 (2010).
[22] Y. Wang, Y. Zheng, C. Xie, and K. Peng, IEEE J. Quantum Electronics **47**, (7), 1006 (2011).
[23] H. Nha, and H. J. Carmichael, Phys. Rev. A **71**, 032336 (2005).
[24] H. Scutaru, J. Phys. A **31**, 3659 (1998).